

RSC Advances



This is an *Accepted Manuscript*, which has been through the Royal Society of Chemistry peer review process and has been accepted for publication.

Accepted Manuscripts are published online shortly after acceptance, before technical editing, formatting and proof reading. Using this free service, authors can make their results available to the community, in citable form, before we publish the edited article. This *Accepted Manuscript* will be replaced by the edited, formatted and paginated article as soon as this is available.

You can find more information about *Accepted Manuscripts* in the [Information for Authors](#).

Please note that technical editing may introduce minor changes to the text and/or graphics, which may alter content. The journal's standard [Terms & Conditions](#) and the [Ethical guidelines](#) still apply. In no event shall the Royal Society of Chemistry be held responsible for any errors or omissions in this *Accepted Manuscript* or any consequences arising from the use of any information it contains.

Cite this: DOI: 10.1039/c0xx00000x

www.rsc.org/xxxxxx

COMMUNICATION

A simple route to synthesize hierarchical porous ZrO₂

Yu Chen,*^a Hui Xia,^a Daiguo Zhang,^a Zilai Yan,^b Fangping Ouyang,^b Xiang Xiong,^b Xiaoyi Huang*^c

Received (in XXX, XXX) Xth XXXXXXXXX 200X, Accepted Xth XXXXXXXXX 200X

DOI: 10.1039/b000000x

A simple method for preparing porous ZrO₂ has been proposed by directly decomposing Zr(NO₃)₄·5H₂O ethanol sol-gel solution. Contrary to other traditional sol-gel methods, porous ZrO₂ with multi-sized Macro- and Meso- pores are synthesized via only one simple step. The size of the macropores is ranged from 100 nm to 500 nm. Remarkably, we also isolated some of highly dispersed ZrO₂ nanoparticles (~ 60 nm), which on their surface or even in the whole body are full filled with well-sized ever-smaller spherical mesopores with an average diameter around ~ 5 nm. A further investigation of low-temperature nitrogen absorption has shown a high surface area over 162 m² g⁻¹ for the fully crystallized ZrO₂. No more additional modifiers or complicated preparations are needed in the present method, which promises a new potential option in fabricating high-porosity materials.

Hierarchical porous metal oxides on multiple scales have attracted considerable attention for both their interesting physical and chemical properties^{1,2}. These types of materials often exhibit high specific surface area, good permeability and low relative density, promising a wide potential application in sensors, catalyzers as well as gas purifications³⁻⁶. Thus, any approaches that could achieve these materials efficiently and inexpensively are of great interests. Up to now, many typical technologies - such as those based on hard or soft templates^{7,8}, self-assembly processes with a help of specific surfactants^{3,9,10}, etc - have been developed to meet this requirement. However, traditional approaches above need either additional modifiers or complicated pre-preparation and post-treating processes. For example, template-based methods need to build a porous framework first, then insert cared materials into the template, and finally remove the pre-created template away if necessary. This is a complicated project and even in its first step, to a large extent, is sometimes a difficult and costly task. In addition, removing the pore-forming frameworks is another big challenge. In contrast, self-assembly processes are comparatively simple. But the method usually requires specific surfactants or pore-forming agents. These surfactants and agents are expensive and how to remove them at the end of the fabrication is also a big problem.

ZrO₂ is one of the most important ceramic materials, which is widely used in oxygen sensors, fuel cells, catalysts and catalyst supports¹¹⁻¹³. These applications can be attributed to its unique physical properties. It is the only traditional metal oxide having both acid and base active centers on its surface, which shows

excellent catalytic activity on some processes of the alkylation and oxidation^{4,14,15}. ZrO₂, as a widely used catalyst or air sensor, requires high specific surface area and strong adsorptive capacity. Increasing the porosity of ZrO₂ or decreasing its particle size is a candidate option. However different from SiO₂, TiO₂, reports on the preparing and manufacturing of porous ZrO₂ are very limited. Fujita et al successfully prepared a porous crystalline zirconia by combining a sol-gel and solvothermal process³. They achieved a high surface area precursor of ZrO₂ gels. However, as mentioned by Fujita et al themselves, the collapse of microstructures in the high temperature of sintering (> 400°C) results in a following great loss of surface area. Hong et al fabricated a ZrO₂ porous ceramic using a camphene-based freeze-casting method⁶. But the method requires some comparatively special preparation conditions and procedures.

Here, we proposed a new and simple method with which hierarchical porous ZrO₂ was fabricated via only one decomposing step of Zr(NO₃)₄·5H₂O ethanol sol-gel solution. In the decomposition products, we found some micron-sized ZrO₂ blocks that full filled with spherical air pores. After a further separation process, we also isolated some of highly dispersed ZrO₂ nanoparticles (~ 60 nm), which on their surface or even in the whole body are full of well-sized ever-smaller spherical mesopores with the average diameter around ~ 5 nm. The successful fabrication of these porous ZrO₂ suggests a new optional approach for preparing high-porosity metal oxides.

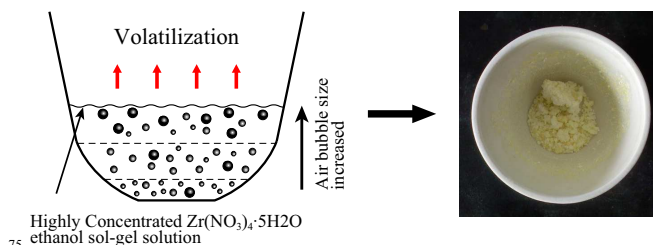


Fig. 1 Schematic representation of the reaction process and the photo of synthesized porous ZrO₂ sample. (a) A illustration of the pore-forming mechanism. The precursor has been concentrated to a very high level, creating a liquid of poor flowability. Air bubbles (with a small size) in this circumstance will be frozen and aggregated where they were created. (b) A photo of amorphous ZrO₂ gels formed at 90 °C.

The entire fabrication process is described as illustrated in Fig. 1(a). The concentration of the sol-gel precursor, chemical reactions to generate porous ZrO₂ gels and the final annealing process were all finished in the same alumina crucible. The new method is, to a large extent, able to avoid the introduction of

unwanted impurities. Furthermore, in order to fabricate a porous ZrO_2 , air bubbles emitted in the thermal decomposition process (NO_2 bubbles) were utilized as a soft template. This kind of soft template also has been successfully applied in the fabricating of porous hierarchical In_2O_3 ¹⁶. The biggest advantage of using air bubbles as a template is that it requires no further treatments at the end of the synthesis. The precursor, however, is another important factor which provides a growth-environment for both air bubbles and ZrO_2 . This requires a liquid of high concentration, low flowability and a fast gelation process accompany with abundant air emission. But the solubility of $\text{Zr}(\text{NO}_3)_4 \cdot 5\text{H}_2\text{O}$ powder in ethanol at room temperature is much lower than this requirement, and there is no significant changes even at the boiling point of this solution. But we found if we firstly prepared a diluent solution, and then let it being volatilized slowly at 60°C , it will be able to form a transparent gel-sol solution with a very high concentration. Thus in this article, 10g $\text{Zr}(\text{NO}_3)_4 \cdot 5\text{H}_2\text{O}$ powder was firstly mixed with 30mL of anhydrous ethanol to form a relatively diluent solution. Then the solution was heated up to 60°C just a little lower than its boiling point and volatilizing at this temperature slowly to achieve a high concentration. As we know, the volatilizing process is usually very slow. Thus we volatilized at 60°C is for the purpose to accelerate this step. The heating rate is well controlled at a very slow speed because present $\text{Zr}(\text{NO}_3)_4$ sol-gel solution is easily to be hydrolyzed directly at a high-speed of heating or if the temperature is higher than 80°C . The reaction process is depicted in Fig. 1(a). As the precursor has been concentrated to a very high level, creating a liquid of poor flowability, air bubbles (with a small size) in this circumstance will be jammed and aggregated where it was created. These air bubbles are emitted simultaneously and utilized as a soft template in the gelation when the temperature reached 90°C . Fig. 1(b) shows the synthesized amorphous ZrO_2 gels.

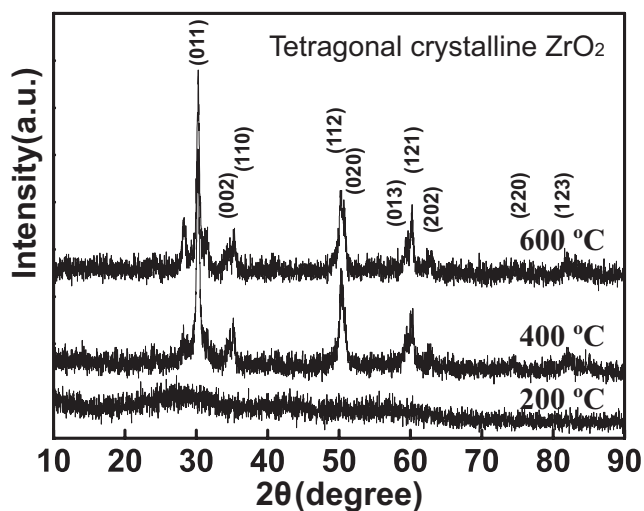


Fig. 2 XRD results of the as-prepared ZrO_2 annealed at different temperature.

The achieved ZrO_2 gels were dried in the air for another 2 hours and then transferred to muffle furnace annealing at different temperature. Figure 2 is the XRD results and shows a tetragonal crystalline ZrO_2 if the sintering temperature is higher than 400°C .

The morphologies and microstructures of the achieved ZrO_2 after crystallization were carefully investigated by FESEM and

the results are shown in Fig. 3. A large area of macro-pores on a micron-sized ZrO_2 block can be clearly observed. It is not a cross-linked air channel as reported in the *Ref. 3*, but regular spherical air bubbles on the surface or embeded inside of the ZrO_2 . Generally, polymerization-induced bicontinuous pores (*in Ref 3*) are easily to be collapsed sintering in high-temperature. However, air bubbles utilized as pore-forming template can be well preserved in present new method (see in Fig. 3). From FESEM images of Fig. 3(c), we can infer that these spherical air pores are not only existed on the materials' surface, but also inside of the ZrO_2 . The size distribution estimated from Fig. 3(b) is ranged from 100 nm to 500 nm. It should be pointed out that this bubble-embedded ZrO_2 is not the only product obtained in the reaction. There are other reactants that have distinct microstructures (please see the details in the supplementaries). In other works, we will focus on the factors, such as pressure, solution concentration, etc, that could determine the formation of pores.

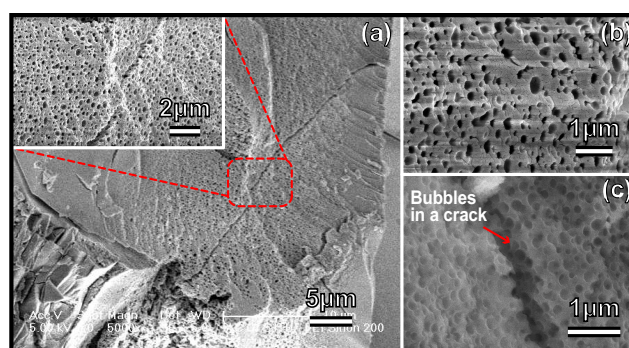


Fig. 3 Morphologies and microstructures of the porous ZrO_2 block. (a) SEM images at a considerable small magnification rate. ZrO_2 block in micron-size was full filled with well-sized spherical pores. The inset is a close-up view of the region selected by the red rounded rectangle. (b) A further magnification of the selected area in (a), from which the pore size distribution can be estimated ranging from 100 nm to 500 nm. (c) A SEM investigation on a crack where bubbles inside of this material can be identified.

The achieved ZrO_2 in the last step was further pulverized into powder by an agate mortar. Remarkably, we isolated some of mesoporous ZrO_2 particles this time. The powder was ultrasonic oscillated in anhydrous ethanol for another 1 hour and then left untouched until a stable and homogeneous suspension was obtained. As we know that pure ethanol has a very low surface tension. Only those materials with high surface area can be suspended stably in this solution. Thus we can infer that the isolated ZrO_2 particles possess a considerable high surface area. A further investigation of the low-temperature nitrogen adsorption has confirmed these conclusions which shows a high BET surface area of over $162 \text{ m}^2 \text{ g}^{-1}$. Figure 5 (a) shows the nitrogen adsorption-desorption isotherm curve. This kind of isotherm indicates the existence of closed pores. A copper grid is then put into the ZrO_2 suspension and lift up for the next SEM and TEM investigations to further examine this assumption. The detailed SEM and FETEM analysis results are shown in Fig. 4. Fig. 4(a) shows SEM images of the highly dispersed ZrO_2 nanoparticles. Red circle selected area was a possible region that will be further characterized using FETEM. The FETEM results are presented in Fig. 4(b)-(f). Nanopores which are spherical and with average diameter around $\sim 5 \text{ nm}$ were founded spreading on

the surface of a comparative bigger ZrO_2 seeds (~ 60 nm). Pore size distribution obtained from nitrogen adsorption data shows that it is centered at 50 Å. In the present experiment, the decomposing process is simultaneously along with the gelation process which emits abundant red-brown NO_2 gases. The emitted NO_2 will form a mass of bubbles in the liquid by the action of surface tension. However, because the liquid at this moment is concentrated to a very high level and the phase transformation is finished so fast that NO_2 bubbles, which have not enough time to be grown up and moved out of the liquid, are frozen and aggregated where they were created and finally to be utilized as a soft pore-forming template. The color of achieved ZrO_2 gels (as show in Fig. 1(b)) are of red-brown at the beginning and beige some hours latter. This phenomenon indicates that ZrO_2 gels have absorbed a considerable amount of NO_2 gases in the gelation. However, after dried in air for some hours, the absorbed NO_2 have finally been released.

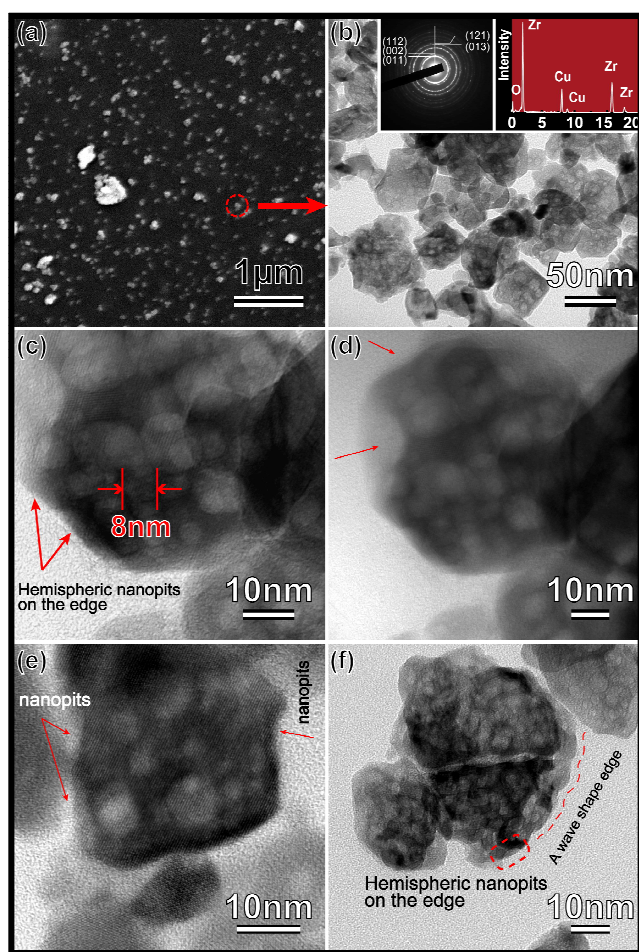


Fig. 4 SEM and TEM analysis of highly dispersed ZrO_2 particles which were isolated from the products in present fabrication. (a) SEM images of the highly dispersed ZrO_2 nanoparticles. Red circle select area is the possible region for the next investigation of TEM. (b) TEM test results in a comparative low magnification. Inset of (b) shows diffraction rings and EDX results of tetragonal ZrO_2 . Copper peaks originate from the TEM sample grid. (c)-(d) HRTEM images of the morphology of one isolated ZrO_2 particle, which sub-nanostructures of spherical nanospots can be clearly observed. Red arrows labeled the irregular edge surface. (e)-(f) Another two distinct ZrO_2 particles which also shown a irregular or a wave shape edge. This phenomena indicates that the surface of these particles are embedded with hemispheric nanospots.

From the results in Figure 4 and 5, we were still unable to confirm whether there are air bubbles or pores embedded inside of these isolated ZrO_2 nanoparticles. But what we can make sure is that hemispheric nanospots are full filled on their surface. Fig. 4(d) is a lower magnification FETEM image for the same particle investigated in Fig. 4(c) which can give a full view of the particle edge. Red arrows in these two figures marked clearly the signs of hemispheric nanospots because of its irregular edge surface. Fig. 4(e) and (f) is the image of another two distinct ZrO_2 nanoparticles. It is indicated that the phenomena of edge surface irregularity is not a single case, but widely existed in these isolated ZrO_2 nanoparticles.

Only Zr, O and Cu (from Cu grid) were detected in the energy dispersive spectrum (EDS) tests (see Fig 4(a)), which confirmed the chemical elements. The electron diffraction pattern (see Fig. 4(a)) matches well with the tetragonal ZrO_2 phase, which the diffraction rings $\{011\}$, $\{002\}$, $\{112\}$, $\{013\}$ and $\{121\}$ has been indexed.

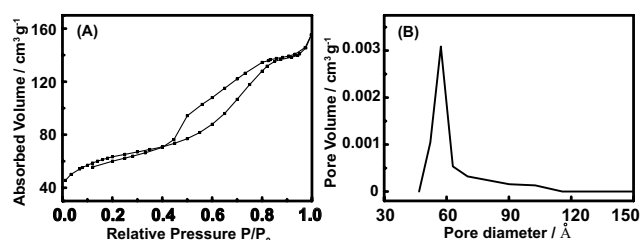


Fig. 5 Nitrogen adsorption characterizations of the isolated porous ZrO_2 powder. (a) Nitrogen adsorption-desorption isotherms. (b) The pore size distribution data.

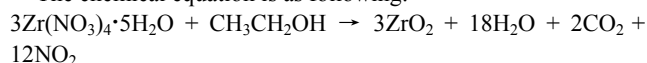
In summary, a novel and simple approach for preparing hierarchical porous ZrO_2 has been proposed using air bubbles as a template. ZrO_2 with multi-sized Macro- and Meso- pores can be easily synthesized via directly decomposing highly concentrated $\text{Zr}(\text{NO}_3)_4 \cdot 5\text{H}_2\text{O}$ ethanol sol-gel solution at 90°C . Air bubbles originated from this fast decomposing process were simultaneously utilized as the soft template. The bulk ZrO_2 material fabricated using this template is full filled with spherical air bubbles and, this bubble framework can still be well preserved even after a high temperature of annealing. Macro-pores analyzed by SEM are ranged from 100 nm to 500 nm. Remarkably, we also isolated some of highly dispersed ZrO_2 nanoparticles (~ 60 nm) which on their surface or even in the whole body are distributed meso-pores with average diameter around ~ 5 nm. No more additional modifiers or complicated preparations are needed in the present method, which promises a new potential option in fabricating porous ZrO_2 .

Methods

Hierarchical porous ZrO_2 are synthesized by directly decomposing highly concentrated ZrO_2 gel-sol solution. The precursor was prepared through dissolving $\text{Zr}(\text{NO}_3)_4 \cdot 5\text{H}_2\text{O}$ in ethanol. The used reagents of $\text{Zr}(\text{NO}_3)_4 \cdot 5\text{H}_2\text{O}$ and alcohol were analytic grade, purchased from Sinopharm Chemical Reagent Shanghai Co., Ltd. Firstly, 10g $\text{Zr}(\text{NO}_3)_4 \cdot 5\text{H}_2\text{O}$ powder was mixed with 30mL of anhydrous ethanol at room temperature. Because of its poor solubility, the $\text{Zr}(\text{NO}_3)_4$ suspending liquid was heated up to 40°C and stirred until it was completely

dissolved. Then in the second step of volatilization, the temperature was raised to 60°C and highly concentrated, transparent ZrO₂ gel-sol solution was achieved after about 1 hour of volatilization. Finally, when ZrO₂ gel-sol solution started to get viscous (total concentration is more than 90%), the temperature was heated up quickly to 90°C. Along with this progress, a large amount of red-brown gas was released and fluffy ZrO₂ (see Figure 1b) filled with hierarchical pores was obtained. After drying two hours in the air, ZrO₂ zirconia was then transferred into muffle furnace for high temperature annealing.

The chemical equation is as following:



The synthesized ZrO₂ after annealing at different temperatures were examined by X-ray diffraction (XRD) measurements on a D/max-2550/PC instrument with a scanning speed of 2 degrees/minute (see Figure 2). FESEM (field emission scanning electron microscope) tests were operated on an FEI Sirion 200 with an acceleration voltage of 5.0 kV. HRTEM (high-resolved transmission electron microscopy) measurements were taken on a JEM-2100f instrument under an acceleration voltage of 200 kV. Energy dispersive X-ray spectra (EDS) were also utilized to confirm the chemical components of the samples. The size distribution of the pore size was calculated from the nitrogen adsorption data using the Barrett-Joyner-Halenda (BJH) method, and the surface area was obtained by the Brunauer-Emmet-Teller (BET) method.

Acknowledgements

This work is financially supported by the National Science Foundation of China (No. 51002009), the Fundamental Research Funds for the Central Universities (No. 2012QNZT055) and Hunan provincial Natural Science Foundation of China (No. 13jj3005). We greatly appreciate the support from Instrumental Analysis Center of Shanghai Jiao Tong University, Shanghai, P. R. China.

References

^a Hunan Key Laboratory for Super-microstructure and Ultrafast Process,

Central South University, 932 Lushan Nan Rd., Changsha, Hunan 410083, P.R. China; E-mail: chenyu_8323@csu.edu.cn

^b Powder Metallurgy Research Institute, and State Key Laboratory of Powder Metallurgy, 932 Lushan Nan Rd., Changsha, Hunan 410083, P.R. China;

^c Physics Department, Xiangnan University, Chenzhou, Hunan 423000, P.R. China; E-mail: jghxy@126.com

† Electronic Supplementary Information (ESI) available:

[1] G.J. Zhang, J.F. Yang, T. Ohji, Fabrication of Porous Ceramics with Unidirectionally Aligned Continuous Pores, *J. Am. Ceram. Soc.*, 84 (2001) 1395-1397.

[2] Z.Y. Yuan, B.L. Su, Insights into Hierarchically Meso/Macroporous Structured Materials, *J. Mater. Chem.*, 16 (2006) 663-667.

[3] J. Konishi, K. Fujita, S. Oiwa, K. Nakanishi, K. Hirao, Crystalline ZrO₂ Monoliths with Well-Defined Macropores and Mesoporous Skeletons Prepared by Combining the Alkoxy-Derived Sol-Gel Process Accompanied by Phase Separation and the Solvothermal Process, *Chem. Mater.*, 20 (2008) 2165-2173.

[4] S. Benfer, E. Knözinger, Structure, morphology and surface properties of nanostructured ZrO₂ particles, *J. Mater. Chem.*, 9 (1999) 1203-1209.

[5] J. Zhou, C.-A. Wang, Porous yttria-Stabilized Zirconia Ceramics Fabricated by Nonaqueous-Based Gelcasting Process with PMMA Microsphere as Pore-Forming Agent, *J. Am. Ceram. Soc.*, 96 (2013) 266-271.

[6] J. Han, C. Hong, X. Zhang, J. Du, W. Zhang, Highly porous ZrO₂ ceramics fabricated by a camphene-based freeze-casting route: Microstructure and properties, *J. Eur. Cer. Soc.*, 30 (2010) 53-60.

[7] M.-L. Wang, C.-H. Wang, W. Wang, Preparation of porous ZrO₂/Al₂O₃ macrobeads from ion-exchange resin templates, *J. Mater. Sci.*, 46 (2011) 1220-1227.

[8] H. Ma, Y. Kong, W. Hou, Q. Yan, Synthesis of Ordered Hexagonal Porous Tin-Doped Zirconium Oxides with a High Surface Area, *Microporous Mesoporous Mater.*, 77 (2005) 241-243.

[9] J. Blin, A. Leonard, Z. Yuan, L. Gigot, A. Vantomme, A. Cheetham, B. Su, Hierarchically Mesoporous/Macroporous Metal Oxides Templated from Polyethylene Oxide Surfactant Assemblies, *Angew. Chem., Int. Ed.*, 42 (2003) 2872.

[10] G. Pacheco, E. Zhao, A. Garcia, A. Sklyarov, J.J. Fripiat, Syntheses of mesoporous zirconia with anionic surfactants, *J. Mater. Chem.*, 8 (1998) 219-226.

[11] Y. Chen, J. Gu, D. Zhang, S. Zhu, H. Su, X. Hu, C. Feng, W. Zhang, Q. Liua, A.R. Parker, Tunable three-dimensional ZrO₂ photonic crystals replicated from single butterfly wing scales, *J. Mater. Chem.*, 21 (2011) 15237-15243.

[12] James F. Haw, Jinhua Zhang, Kiyoyuki Shimizu, T. N. Venkatraman, Donat-Pierre Luigi, Weiguo Song, Dewey H. Barich and John B. Nicholas, NMR and Theoretical Study of Acidity Probes on Sulfated Zirconia Catalysts, *J. Am. Chem. Soc.*, 122 (2000) 12561.

[13] I.J. Dijs, J.W. Geus, L.W. Jenneskens, Effect of Size and Extent of Sulfation of Bulk and Silica-Supported ZrO₂ on Catalytic Activity in Gas- and Liquid-Phase Reactions, *J. Phys. Chem. B*, 107 (2003) 13403-13413.

[14] T. Yamagushi, Application of ZrO₂ as a catalyst and a catalyst support, *Catal. Today*, 20 (1994) 199.

[15] R. Takahashi, S. Sato, T. Sodesawa, K. Suzuki, M. Tafu, K. Nakanishi, N. Soga, Phase Separation in Sol-Gel Process of Alkoxide-Derived Silica-Zirconia in the Presence of Polyethylene Oxide, *J. Am. Ceram. Soc.*, 84 (2001) 1968-1976

[16] Ligang Gai, Li Ma, Haihui Jiang, Yun Ma, Yan Tian and Hong Liu, Nitrogen-doped In₂O₃ nanocrystals constituting hierarchical structures with enhanced gas-sensing properties, *Crystrngcomm*, 14 (2012) 7479-7486.